ELSEVIER

Journal of Alloys and Compounds 216 (1994) 99–103

Journal of ALLOYS AND COMPOUNDS

Dielectric constant and conductivity of $Er_2Cu_2O_5$

G. Knebel[a], P. Lunkenheimer[a,*], A. Loidl[a], G. Wltschek[b], H. Fuess[b]

[a]*Institut für Festkörperphysik, Technische Hochschule Darmstadt, D-64289 Darmstadt, Germany*

[b]*Fachbereich Materialwissenschaft, Technische Hochschule Darmstadt, D-64287 Darmstadt, Germany*

Received 8 April 1994

Abstract

Structural data, electrical transport and dielectric properties are reported for $Er_2Cu_2O_5$. Similar to La_2CuO_4, this cuprate oxide reveals a two-dimensional CuO_2 network. At low temperatures and high frequencies the electrical transport is dominated by hopping conductivity processes. The dielectric constant $\varepsilon \approx 9.0(5)$ has been determined from high frequency measurements. At high temperatures and low frequencies d.c. conductivity contributions dominate and characterize $Er_2Cu_2O_5$ as a conventional semiconductor with a gap $E_G = 1.4$ eV.

Keywords: Dielectric properties; Conductivity; Cuprate oxides

1. Introduction

The discovery of the superconducting cuprates has led to intensive studies of related (non-superconducting) copper oxides. In the ternary R–Cu–O phase diagram (R denotes a rare earth element) only the compounds with a composition $R_2Cu_2O_5$ are stable for rare earth ions smaller than Gd^{3+} [1]. These materials crystallize in the orthorhombic $Ho_2Cu_2O_5$ structure (space group $Pna2_1$) [2]. Similar to the high T_c superconductors, low dimensional copper oxide structures do exist in these materials. Four oxygen atoms form a distorted square with a central Cu ion. Each two of these squares share one edge and are linked together by corners to form zigzag chains along the [100] direction. Up to now considerable work has been done on the magnetic properties of $Er_2Cu_2O_5$ [3,4]. The Cu and Er moments order simultaneously at $T_N = 27.5$ K. The copper moments order collinearly parallel to [010], whereas the erbium moments order coplanarly in the *bc* plane [5]. However, to our knowledge, investigations of the electrical transport properties of $Er_2Cu_2O_5$ are still lacking. Especially interesting would be the comparison with the "parent" compounds of the superconducting cuprates, La_2CuO_4 and $YBa_2Cu_3O_6$, for which hopping conductivity has been found as the dominant charge transport mechanism [6–9]. In addition, La_2CuO_4 reveals an unusually large dielectric constant [6,10] and even at high temperatures no evidence of a large gap of about 2 eV, as inferred from optical experiments, could be detected in resistivity experiments [11].

We investigated the a.c. conductivity σ and the dielectric constant ε of $Er_2Cu_2O_5$. The measurements were carried out in a broad frequency range, 20 Hz $\leqslant \nu \leqslant$ 4 GHz, and at temperatures $150 \leqslant T \leqslant 500$ K. From the frequency dependence of σ and ε we found clear evidence for hopping conductivity in $Er_2Cu_2O_5$. The high frequency data allowed a precise determination of the dielectric constant ε_∞. From the low frequency and high temperature results the d.c. conductivity was determined, from which we calculated the semiconducting energy gap E_G.

2. Experimental details

The synthesis of erbium cuprate, $Er_2Cu_2O_5$, was carried out by subsolidus reaction of stoichiometric mixtures of erbium sesquioxide, Er_2O_3 (99.99% Aldrich), and copper oxide, CuO (99.99% Aldrich), in the ratio 1:2. All reactants were mixed in an agate mortar under acetone and heated at 1223 K in flowing oxygen (0.5 l h^{-1}) for 24 h. Afterwards the reaction product was cooled at 120 K h^{-1} to room temperature. The resulting $Er_2Cu_2O_5$ ceramics were studied with synchroton radiation. The structure was determined by Patterson synthesis and refined by Rietveld analysis. The resulting lattice parameters were $a = 10.7344(4)$, $b = 3.4577(5)$ and $c = 12.3961(3)$ Å. Table 1 gives the refined values for the atomic positions in the unit cell. Fig. 1 shows the

*Corresponding author.

SSDI 0925-8388(94)01253-E

Table 1
Crystallographic data of $Er_2Cu_2O_5$ at 298 K

Atom	x	y	z
Er(1)	0.2099(3)	0.2250(6)	0.00000
Er(2)	0.0452(3)	0.2234(6)	0.3301(2)
Cu(1)	0.9856(6)	0.6546(16)	0.1082(2)
Cu(2)	0.2550(6)	0.6597(4)	0.2119(3)
O(1)	0.185(5)	0.695(6)	0.365(10)
O(2)	0.336(4)	0.721(8)	0.048(4)
O(3)	0.134(3)	0.328(6)	0.167(3)
O(4)	0.427(4)	0.756(8)	0.245(4)
O(5)	0.424(3)	0.239(9)	0.488(2)

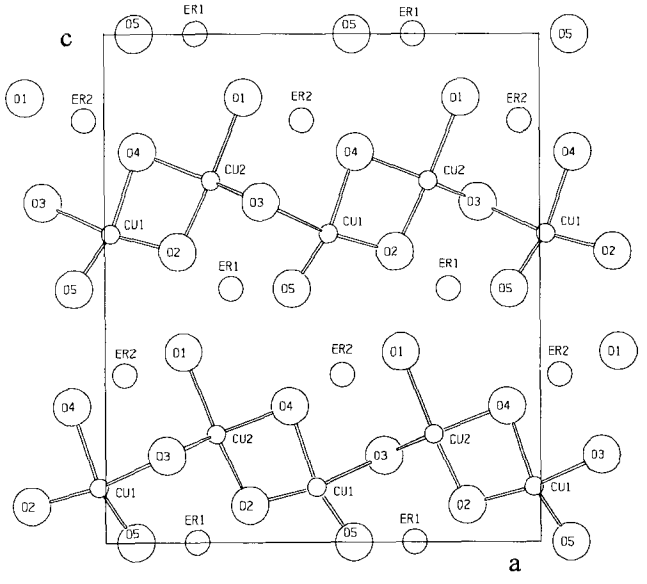

Fig. 1. The *ca* plane of $Er_2Cu_2O_5$ showing the low dimensional CuO structures.

planar network of CuO in the *ac* plane. No spurious phases could be detected. The samples were characterized utilizing a.c. susceptibility measurements, yielding an antiferromagnetic ordering temperature $T_N = 27.2$ K. A Curie–Weiss fit to the paramagnetic susceptibility below $T = 100$ K revealed a Curie–Weiss temperature $\Theta = -16$ K and an effective moment $\mu_{eff} = 6.9\ \mu_B$.

To study the electrical properties of the $Er_2Cu_2O_5$ ceramics, silver paint has been applied to opposite sides of the pellets as contacts. To determine the real part ε' and imaginary part ε'' of the dielectric constant or correspondingly the imaginary part σ'' and the real part σ' of the complex conductivity in a broad frequency range, various measuring techniques have been employed. For frequencies 20 Hz $\leqslant \nu \leqslant$ 1 MHz a fully automated autobalance bridge (HP4284) has been used. To carry out temperature-dependent measurements, the sample has been mounted in a gas-heating system and connected to the bridge by four coaxial cables in order to avoid cable contributions. For higher frequencies $\nu \geqslant 1$ MHz the sample has been placed at the end of a coaxial line, thereby connecting the inner and outer conductor. The complex reflection coefficient Γ of this assembly has been measured using an HP4191 impedance analyser for frequencies 1 MHz $\leqslant \nu \leqslant 1$ GHz and an HP8510 network analyser for $\nu > 1$ GHz. From Γ the electrical properties of the sample can be calculated after a proper calibration using three standard samples to eliminate the influence of the coaxial line and sample holder. The high frequency measurements have been carried out at room temperature only. Because all measurements have been performed utilizing two-point contact techniques, one has to take care of possible contact contributions. However, measurements of samples with different geometries gave identical results for σ' and ε', justifying the assumption that the (additive) contact resistances can be neglected. Moreover, we measured the d.c. resistance of our samples at room temperature by a four-point technique using an electrometer. The results agreed well with the extrapolated d.c. resistance from our two-point measurements.

3. Results and discussion

Fig. 2 shows the real part of the dielectric constant, ε', and the real part of the conductivity, $\sigma' = \omega\varepsilon_0\varepsilon''$ (with $\omega = 2\pi\nu$ and ε_0 the permittivity of free space), for frequencies 10 Hz $\leqslant \nu \leqslant$ 4 GHz at room temperature. $\varepsilon'(\nu)$ is frequency independent for $\nu > 1$ MHz, reaching the limiting value of the dielectric constant $\varepsilon_\infty = 9$. The increase in ε' towards low frequencies indicates that hopping processes of charge carriers dominate [12,13]. In a log–log representation $\sigma'(\nu)$ follows a straight line with slope $s = 0.67$ over eight decades of frequency. (The slight deviations at $\nu > 2.5$ GHz can be ascribed to a slightly imperfect calibration of the HP8510 network analyser due to differences in the geometries of sample and calibration standard.) Hence the dielectric loss (or σ') is determined solely by hopping or tunnelling of localized charge carriers for all frequencies [12,13].

Fig. 3 shows the temperature dependence of the real part of the a.c. conductivity, σ'_{ac} (closed symbols), for various frequencies in an Arrhenius representation $\log_{10}(\sigma')$ vs. $1000/T$. Also included is the d.c. conductivity σ_{dc} (open circles) obtained from fits to the frequency dependence of σ' as described below. $\sigma_{ac}(T)$ exhibits clear deviations from Arrhenius behaviour. For high temperatures and low frequencies σ_{ac} reaches the d.c. limit. $\sigma_{dc}(T)$ can well be described by the behaviour of an intrinsic semiconductor, $\sigma_{dc} \propto \exp(-E/2k_BT)$ with $E \approx 1.4$ eV (solid line in Fig. 3).

Fig. 4 shows the frequency dependence of σ' (bottom) and ϵ' (top) for various frequencies. The conductivity follows a power law $\sigma \propto \nu^s$ with $s < 1$, as can be seen clearly in the log–log representation of Fig. 4. For high

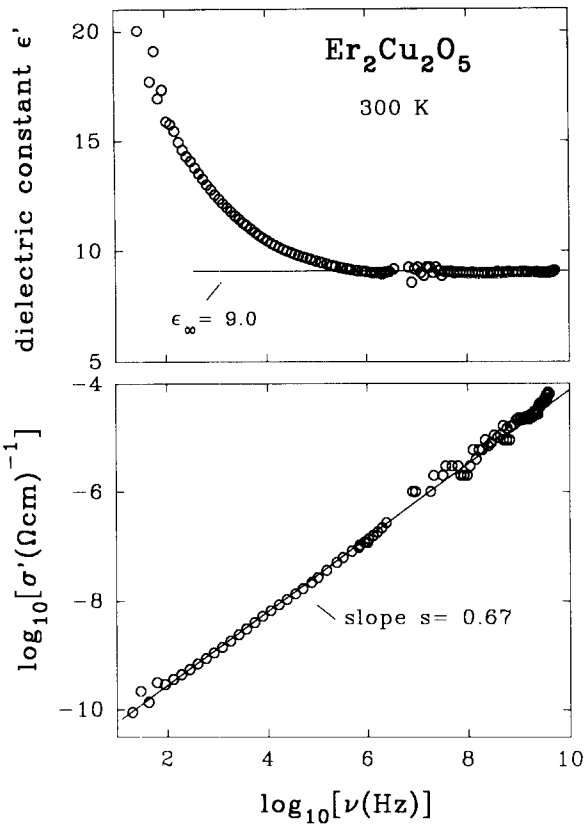

Fig. 2. Frequency dependence of the real parts of the dielectric constant, ε' (top), and the conductivity σ' (bottom), at room temperature, including results up to 4 GHz. At the top the high frequency dielectric constant is indicated. At the bottom a straight line has been included demonstrating that $\sigma'(\nu)$ follows a power law $\sigma' \propto \nu^s$ with s constant over eight decades of frequency.

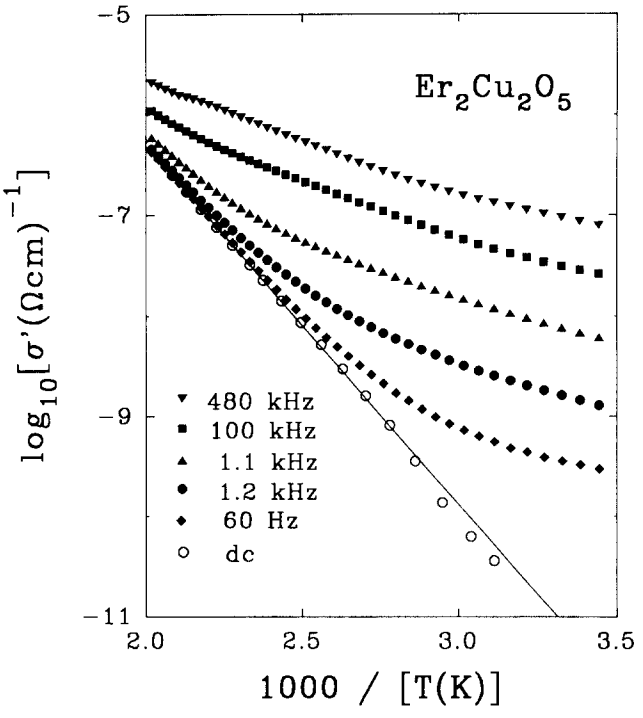

Fig. 3. Temperature dependence of the real part of the conductivity, σ', in Arrhenius representation for various frequencies (closed symbols). The open circles denote the d.c. conductivity as obtained from fits to $\sigma(\nu)$ (see text). The solid line is the result of a fit to $\sigma_{dc}(T)$ using an Arrhenius law.

temperatures σ' approaches a constant value for $\nu \to 0$ which can be identified with σ_{dc}. Such a behaviour has been found in a large number of materials, including amorphous and crystalline semiconductors, ionic conductors, polymers, etc. [12], and is a fingerprint of hopping conductivity. There is a vast number of theoretical approaches to deduce the observed ν^s dependence of σ' from the microscopic transport properties of various classes of materials. Processes involving hopping over or tunnelling through an energy barrier separating different localized defect states have been considered for various kinds of charge carriers, e.g. electrons, polarons, ions, etc. [13]. However, common to all theories is the result that $\sigma' \propto \nu^s$, which holds true at least in a limited frequency range. An *exact* ν^s behaviour (i.e. with a frequency-independent s) is known as the "universal dielectric response" [12] and has been found for most hopping systems. Within this model ε' and σ' can be calculated as

$$\sigma' = \sigma_{dc} + \sigma_0 \omega^s$$

$$\epsilon' = \frac{\tan(s\pi/2)\sigma_0 \omega^{s-1}}{\varepsilon_0 + \varepsilon_\infty}$$

Here ε_∞ has been included to take into account the high frequency dielectric constant of the sample.

Least-squares fits using these formulae have been carried out simultaneously for $\epsilon'(\nu)$ and $\sigma'(\nu)$ and are shown as solid curves in Fig. 4. A good agreement between data and fit could be achieved. In fitting $\epsilon'(\nu)$, points below 100 Hz have not been used because the data scatter strongly in this range. For high frequencies $\varepsilon'(\nu)$ approaches the frequency- and almost temperature-independent ε_∞. The fits yield $\varepsilon_\infty = 9.0$, in good agreement with the high frequency results. The frequency exponent $s(T)$ is almost constant, with a slight tendency to increase with decreasing T (inset in Fig. 4). A temperature-independent s is predicted for thermally assisted tunnelling between localized states [13]. Below 290 K (data not shown) it is difficult to determine s exactly owing to the low conductivity (leading to a strong scatter in the data) and because of the dominance of ε_∞ in $\varepsilon'(\nu)$ at low temperatures. Therefore it is difficult to get information on the temperature dependence of s below 290 K from our data. σ_{dc} resulting from the fits has been included in Fig. 3 as mentioned above. Below room temperature a determination of σ_{dc} from our data is impossible.

Finally we want to compare the results on $Er_2Cu_2O_5$ with some "parent" compounds of the high T_c superconductors. Among them La_2CuO_4 is the most thoroughly studied material. It exhibits an unusually large

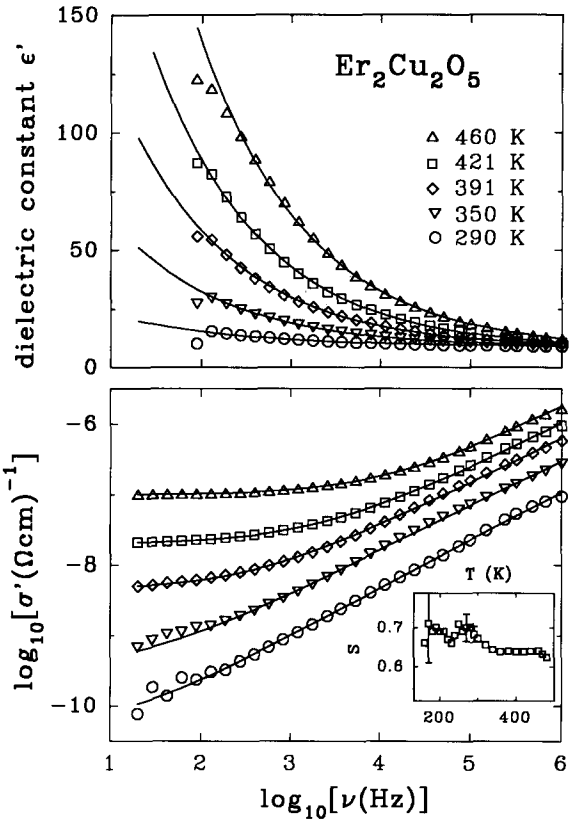

Fig. 4. Frequency dependence of the real parts of the dielectric constant, ε' (top), and the conductivity, σ' (bottom), at various temperatures. The solid curves are fits carried out simultaneously for $\varepsilon'(\nu)$ and $\sigma'(\nu)$ using the universal dielectric response (see text). The resulting temperature dependence of the frequency exponent s is shown in the inset.

dielectric constant $\varepsilon_{ab} > 30$ parallel to the *ab* plane and $\varepsilon_c \approx 25$ along the *c* axis [6,10]. Large dielectric constants, namely $\varepsilon_{ab} \approx 32$ and $\varepsilon_c \approx 23$, were also detected in $EuBa_2Cu_3O_6$ [10], while in $YBa_2Cu_3O_6$ ε is significantly smaller and amounts to approximately 15 as measured in ceramic samples [8]. The large values of ε have been attributed to a close coupling of the atomic motion to electronic charge transfer processes [10] or to the formation of large polarons [6]. Such a coupling seems to be absent in $Er_2Cu_2O_5$ and the dielectric constant $\varepsilon \approx 9$ is rather "normal" as compared with other semiconducting materials. According to a very simplified model of the dielectric properties of semiconducting materials, $\varepsilon \propto (\hbar\omega_p/E_G)^2$, where ω_p is the plasma frequency [14], and indeed there is a trend of increasing ε with decreasing gap energy for a broad class of semiconductors. The values of E_G and ε for $Er_2Cu_2O_5$ also satisfy this relation.

Concerning the d.c. conductivity of the parent materials, the experimental situation is not clear. In $YBa_2Cu_3O_6$ a heavily sample-dependent $\sigma_{dc}(T)$ has been found which deviates clearly from a thermally activated behaviour. In La_2CuO_4 $\sigma_{dc} \propto \exp[(T/T_0)^\gamma]$ with $\gamma = \frac{1}{3}$ or $\frac{1}{4}$. This is characteristic for amorphous semiconductors and can be described by Mott's variable-range hopping (VRH) theory [15]. For some samples the VRH mechanism extends up to room temperature [7,11], while other samples reveal a transition to a thermally activated behaviour close to 50 K [11,16]. The activation energy amounts to 24–70 meV, which is in clear contrast with the gap energy of $E \approx 2$ eV as inferred from optical experiments [17] but would be in agreement with the large dielectric constant. In $Er_2Cu_2O_5$ we found purely activated behaviour above 300 K with a room temperature conductivity of $\sigma_{dc}(300K) \approx 10^{-11}\ \Omega^{-1}\ cm^{-1}$. This value is many decades smaller than $\sigma_{dc}(300\ K) \approx 0.2\text{–}1\ \Omega^{-1}\ cm^{-1}$ for La_2CuO_4 [11,16] and $\sigma_{dc}(300\ K) \approx (2\text{–}4) \times 10^{-3}\ \Omega^{-1}\ cm^{-1}$ for $YBa_2Cu_3O_6$ [9]. From our experiments $Er_2Cu_2O_5$ can be characterized as a conventional semiconductor with a band gap of 1.4 eV. In comparison, the situation in La_2CuO_4 is much less clear as mentioned above. The high ε_∞ in La_2CuO_4 may be predominantly due to ionic or polaronic processes [6] and the low gap in La_2CuO_4 could indicate that the Fermi energy and the mobility edge are close to the upper bound of the lower Mott–Hubbard (or charge transfer) band.

4. Summary and conclusions

$Er_2Cu_2O_5$ has been investigated by dielectric techniques in a broad frequency and temperature range. It can be characterized as a semiconductor with a gap energy $E_G = 1.4$ eV. The dielectric constant $\varepsilon_\infty = 9.0$. The a.c. conductivity is dominated by hopping processes following a power law $\sigma' \propto \nu^s$ with $s \approx 0.65$; s is only weakly temperature dependent. $\sigma'(\nu)$ and $\varepsilon'(\nu)$ can be well described by the universal dielectric response. The frequency exponent s is constant over eight decades of frequency.

References

[1] O. Schmitz-Dumont and H. Kasper, *Monatsh. Chem., 96* (1965) 506.

[2] H.R. Freund and H. Müller-Buschbaum, *Z. Naturf. B, 32* (1977) 609.

[3] R. Troc, J. Klamut, Z. Bukowski, R. Horyn and J. Steppien-Damm, *Physica B, 154* (1989) 189.
Ya. Zoubkova, Z.A. Kazei, R.Z. Levitin, B.V. Mill, V.V. Moshchalkov and V.V. Snegirev, *JETP Lett., 49* (1989) 606.
Z.A. Kazei, N.P. Kolmakova, R.Z. Levitin, B.V. Mill, V.V. Moshchalkov, V.N. Orlov, V.V. Snegirev and Ya. Zoubkova, *J. Magn. Magn. Mater., 86* (1990) 124.

[4] J.L. Garcia-Munoz, J. Rodriguez-Carvajal, X. Obradors, M. Vallet-Regi, J. Gonzalez-Calbet and M. Parras, *Phys. Rev. B, 44* (1991) 4716.
V.P. Plakhtii, M. Bonnet, I.V Golosovskii, B.V. Mill, E. Roudeau and E.I. Fedorova, *JETP Lett., 51* (1990) 723.

[5] G. Wltschek, H. Ehrenberg and H. Fuess, in preparation.

[6] C.Y. Chen, R.J. Birgeneau, M.A. Kastner, N.W. Preyer and T. Thio, *Phys. Rev. B, 43* (1991) 392.

[7] P. Lunkenheimer, M. Resch, A. Loidl and Y. Hidaka, *Phys. Rev. Lett., 69* (1992) 498.

[8] G.A. Samara, W.F. Hammetter and E.L. Venturini, *Phys. Rev. B, 41* (1990) 8974.

[9] C.M. Rey, H. Mathias, R.L. Testardi and S. Skirius, *Phys. Rev. B, 45* (1992) 10 639.

[10] D. Reagor, A. Migliori, S.W. Cheong and Z. Fisk, *Physica B, 163* (1990) 264.

[11] M.A. Kastner, R.J. Birgeneau, C.Y. Chen, Y.M. Chiang, D.R. Gabbe, H.P. Jenssen, T. Junk, C.J. Peters, P.J. Picone, T. Thio, T.R. Thurston and H.L. Tuller, *Phys. Rev. B, 37* (1988) 111.

[12] A.K. Jonscher, *Dielectric Relaxations in Solids,* Chelsea Dielectrics Press, London, 1983.

[13] A.R. Long, *Adv. Phys., 31* (1982) 553.
S.R. Elliott, *Adv. Phys., 36* (1987) 135.

[14] J.C. Phillips, *Bond and Bands in Semiconductors,* Academic Press, New York, 1973.

[15] N.F. Mott and E.A. Davies, *Electronic Processes in Non-Crystalline Materials,* Oxford University Press, Oxford, 1971.

[16] J. Tateno, N. Masaki and A. Iwase, *Phys. Lett. A, 138* (1989) 313.

[17] J. Orenstein, G.A. Thomas, D.H. Rapkine, C.G. Bethea, B.F. Levine, R.J. Cava, E.A. Rietman and D.W. Johnson, *Phys. Rev. B, 36* (1987) 729.
S.L. Herr, K. Kamaras, C.D. Porter, M.G. Doss, D.B. Tanner, D.A. Bonn, J.E. Geedan, C.V. Stager and T. Timsuk, *Phys. Rev. B, 36* (1987) 733.
J.P. Falck, A. Levy, M.A. Kastner and R.J. Birgeneau, *Phys. Rev. Lett., 69* (1992) 1109.